J Physiol 588.18 (2010) pp 3385–3396

The Journal of Physiology

Molecular determinants of hyperosmotically activated NKCC1-mediated K^+/K^+ exchange

Kenneth B. Gagnon and Eric Delpire

Department of Anesthesiology, Vanderbilt University School of Medicine, Nashville, TN 37232, USA

Na^+–K^+–$2Cl^-$ cotransport (NKCC) mediates the movement of two Cl^- ions for one Na^+ and one K^+ ion. Under isosmotic conditions or with activation of the kinases SPAK/WNK4, the NKCC1-mediated Cl^- uptake in *Xenopus laevis* oocytes, as measured using ^{36}Cl, is twice the value of K^+ uptake, as determined using ^{86}Rb. Under hyperosmotic conditions, there is a significant activation of the bumetanide-sensitive K^+ uptake with only a minimal increase in bumetanide-sensitive Cl^- uptake. This suggests that when stimulated by hypertonicity, the cotransporter mediates K^+/K^+ and Cl^-/Cl^- exchange. Although significant stimulation of K^+/K^+ exchange was observed with NKCC1, a significantly smaller hyperosmotic stimulatory effect was observed with NKCC2. In order to identify the molecular determinant(s) of this NKCC1-specific activation, we created chimeras of the mouse NKCC1 and the rat NKCC2. Swapping the regulatory amino termini of the cotransporters neither conferred activation to NKCC2 nor prevented activation of NKCC1. Using unique restrictions sites, we created additional chimeric molecules and determined that the first intracellular loop between membrane-spanning domains one and two and the second extracellular loop between membrane-spanning domains three and four of NKCC1 are necessary components of the hyperosmotic stimulation of K^+/K^+ exchange.

(Received 21 April 2010; accepted after revision 2 June 2010; first published online 7 June 2010)

Corresponding author E. Delpire: Department of Anesthesiology, Vanderbilt University Medical Center, T-4202 Medical Center North, 1161 21st Ave South, Nashville, TN 37232-2520, USA. Email: eric.delpire@vanderbilt.edu

Abbreviations ECL, extracellular loop; ICL, intracellular loop; TMD, transmembrane domain.

Introduction

Mammalian genes *SLC12A2* and *SLC12A3* encode NKCC1 and NKCC2, two transport mechanisms promoting the electroneutral-coupled movement of Na^+ and K^+ with Cl^-. Cation–chloride cotransport is active in a variety of epithelia, where it facilitates the trans-epithelial movement of ions and fluid. NKCC2 is expressed in the kidney's thick ascending loop of Henle, where it mediates the reabsorption of salts, thus contributing to the maintenance of whole body ion and water homeostasis and controlling blood pressure (Kaplan *et al.* 1996). NKCC1, in contrast, is expressed in salt- and fluid-secreting epithelia. Some examples are the salivary (Kurihara *et al.* 2002), lacrimal (Ozawa *et al.* 1988; Douglas & Brown, 1996) and sweat glands (Sato *et al.* 1989), the airway (Liedtke, 1989; Haas *et al.* 1995), intestinal (Matthews *et al.* 1994) and inner ear epithelia (Delpire *et al.* 1999). In neurons, NKCC1 is highly expressed in olfactory neurons (Reisert *et al.* 2005) and dorsal root ganglion neurons (Alvarez-Leefmans *et al.* 1988; Plotkin *et al.* 1997; Sung *et al.* 2000), where it accumulates intracellular Cl^-, thereby facilitating GABA depolarization. In the spinal cord, depolarization of primary afferent fibre terminals by interneurons leads to presynaptic inhibition which affects the gating or transmission of somatosensory signals (Alvarez-Leefmans, 2009).

NKCC1 has also been shown to participate in the maintenance and regulation of cell volume (Hoffmann *et al.* 2009). The osmotic sensitivity of NKCC1 was recognized at the time of its initial functional identification some 30 years ago. Activation of the cotransporter has been demonstrated both by hypertonicity and cell shrinkage (for reviews, see Russell, 2000; Hoffmann *et al.* 2009). Interestingly, although both NKCC1 and NKCC2 are activated by hypertonicity, NKCC1 activation is several-fold greater (Schmidt & McManus, 1977*a*; Geck *et al.* 1980; Geck & Pfeiffer, 1985) than that of NKCC2 activation (Gimenez & Forbush, 2005). The physiological

DOI: 10.1113/jphysiol.2010.191932

relevance of the high osmotic sensitivity of NKCC1 is not yet understood, neither in epithelia nor in sensory neurons.

An important feature of Na^+–K^+–$2Cl^-$ cotransport is that its activity is closely related to its state of phosphorylation (Lytle, 1997). One possible model of Na^+–K^+–$2Cl^-$ cotransport activation could be a binary model in which the non-phosphorylated cotransporter would be inactive and become active upon phosphorylation. The basal activity level of Na^+–K^+–$2Cl^-$ cotransport in cells would then be determined by the number of transporters existing in their active or phosphorylated state. Note that this two-state model (phosphorylated *versus* dephosphorylated) is not incompatible with the fact that several serine/threonine residues are phosphorylated upon activation (Darman & Forbush, 2002; Moriguchi *et al.* 2006; Vitari *et al.* 2006; Gagnon *et al.* 2007) and the possibility that multiple kinases might be involved in the activation (Klein *et al.* 1999; Wong *et al.* 2001; Darman & Forbush, 2002; Gagnon *et al.* 2006*a*). In an alternative model, phosphorylation of specific residues could lead to different levels of cotransporter activation, much like having multiple activation gears. Existing data do not favour one model of activation over another.

Two kinases, Ste20 proline–alanine-rich kinase (SPAK) and oxidative stress-response kinase (OSR1), have been shown to directly phosphorylate NKCC1 (Gagnon *et al.* 2006*a*; Moriguchi *et al.* 2006; Vitari *et al.* 2006) and NKCC2 (Gimenez & Forbush, 2005). These kinases belong to the family of mammalian Ste20-like protein kinases (Dan *et al.* 2001; Delpire, 2009). To activate the transporters, the kinases use a specific domain formed by the last 90 residues of their C-terminus to anchor themselves to their target. This protein fold recognizes specific RF*x*[V/I] (Arginine (R) Phenylananine (F) any amino acid (x) and Valine or Isoleucine (V/I)) peptide sequences that are located in the cytosolic N-terminal domain of the cotransporters (Piechotta *et al.* 2002; Villa *et al.* 2007). After binding, the kinases phosphorylate specific conserved threonine residues that are located downstream of the binding site.

It is unlikely that the difference in osmotic sensitivity between NKCC1 and NKCC2 could be explained on the basis of different effects of kinase phosphorylation and activation. Indeed, both proteins contain SPAK/OSR1 binding sites and have a high degree of conservation in their phosphorylation segments. It is more likely that structural differences exist between the two cotransporters that account for their different responses to osmolarity. On that assumption, we created chimeras of the mouse NKCC1 and the rat NKCC2 in order to identify the molecular determinant(s) of this NKCC1-specific sensitivity to osmolarity.

Methods

Cloning of *Xenopus laevis* NKCC1

Three sets of sense and antisense oligonucleotide primers were designed based on *Xenopus laevis* expressed sequence tags (ESTs) deposited in the National Center for Biotechnology Information database. Complementary DNA was reverse transcribed from RNA isolated from 10 defolliculated oocytes, and high-fidelity, long-range PCR was used to amplify three overlapping pieces of the open reading frame of *Xenopus* NKCC1. After separation of the PCR reactions using 1% agarose gel electrophoresis, each cDNA band was extracted and ligated into the TA cloning vector pGEM-Teasy (Invitrogen, Carlsbad, CA, USA). Several clones of each fragment were sequenced to verify that they were free of mutations. A full-length NKCC1 clone was then assembled using unique SphI and BamHI restriction sites and inserted into the *Xenopus laevis* expression vector pBF using EcoRI–NotI restriction sites.

Construction of mouse NKCC chimeras

We moved fragments of the mouse NKCC1 and rat NKCC2 into pBluescript as templates for QuikChange Mutagenesis (Strategene, La Jolla, CA, USA). Using complementary sense and antisense oligonucleotides, unique restriction sites already present in NKCC1 were introduced into NKCC2 (and vice versa) to allow swapping of sections of each molecule with the other (see Fig. 1). We also used site-directed mutagenesis to change NKCC1 specific residues into NKCC2 residues within the chimeric constructs. All mutations were verified by DNA sequencing and then the full-length NKCC1–NKCC2 chimeras were inserted into pBF with EcoRI–XhoI restriction enzymes.

cRNA synthesis

All cDNA clones in pBF were linearized with MluI and transcribed into cRNA using Ambion's mMESSAGE mMACHINE SP6 transcription system (Ambion, Austin, TX, USA). RNA quality was verified by gel electrophoresis (1% agarose–0.693% formaldehyde) and quantitated by measurement of absorbance at 260 nm.

Isolation of *Xenopus laevis* oocytes

Stage V–VI *Xenopus laevis* oocytes were isolated from 12 different frogs as previously described (Gagnon *et al.* 2006*b*, 2007) and maintained at 16°C in modified L15 medium (Leibovitz's L15 solution diluted with water to a final osmolarity of 195–200 mosmol l^{-1} and

supplemented with 10 mM Hepes and 44 μg gentamicin sulphate). Oocytes were injected on day 2 with 50 nl water containing 15 ng wild-type NKCC1, wild-type NKCC2 or chimeric NKCC1–NKCC2 cRNA. Control oocytes were injected with 50 nl water. Tracer uptakes were performed on day 5 post-isolation.

K^+ uptakes in *Xenopus laevis* oocytes

Groups of 20–25 oocytes in a 35 mm dish were washed once with 3 ml isosmotic saline (96 mM NaCl, 4 mM KCl, 2 mM $CaCl_2$, 1 mM $MgCl_2$, 5 mM Hepes buffered to pH 7.4, 195–200 mosmol l^{-1}) and pre-incubated for 15 min in 1 ml of the same isosmotic saline containing 1 mM ouabain. The solution was then aspirated and replaced with 1 ml isosmotic flux solution containing 5 μCi ^{86}Rb (Perkin Elmer Life Science Inc., Boston, MA, USA). Two 5 μl aliquots of flux solution were sampled at the beginning of each ^{86}Rb uptake period and used as standards. After 1 h uptake, the radioactive solution was aspirated and the oocytes were washed 4 times with 3 ml ice-cold isosmotic solution. Hyperosmotic saline (260–265 mosmol l^{-1}) was obtained by adding 65 mM sucrose to the isosmotic saline. Single oocytes were transferred into glass vials, lysed for 1 h with 200 μl 0.25 N NaOH, neutralized with 100 μl glacial acetic acid and ^{86}Rb tracer activity was measured by β-scintillation counting. NKCC1 flux is expressed in nanomoles K^+ per oocyte per hour.

Co-determination of K^+ and Cl^- uptakes in *Xenopus laevis* oocytes

^{36}Cl was purchased from American Radiolabeled Chemicals, Inc. (St Louis, MO, USA). The isotope arrived as a ~pH 2 solution containing 541 mM NaCl; therefore, we modified our isosmotic saline to contain 66 mM NaCl, 4.1 mM KCl, 2 mM $CaCl_2$, 1 mM $MgCl_2$, 10 mM Hepes, 20 mM Tris, buffered to pH 7.4 In this way, addition of either 20 μl of 541 mM NaCl (for pre-incubation or ^{86}Rb uptake) or 20 μl ^{36}Cl per millilitre maintained isotonicity (195–200 mosmol l^{-1}). Groups of 20–25 oocytes in a 35 mm dish were washed once with 3 ml isosmotic saline and pre-incubated for 15 min in 1 ml of the same isomotic saline containing 1 mM ouabain. The solution was then aspirated and replaced with 1 ml isomotic flux solution containing either 5 μCi ^{86}Rb or 2 μCi ^{36}Cl. Two 5 μl aliquots of flux solution were sampled at the beginning of each isotope uptake period and used as standards. After 1 h uptake, the radioactive solution was aspirated and the oocytes were washed 4 times with 3 ml ice-cold isosmotic solution. Hyperosmotic saline (260–265 mosmol l^{-1}) was obtained by adding 65 mM sucrose to the isosmotic saline. Single oocytes were transferred into glass vials, lysed for 1 h with 200 μl 0.25 N NaOH, neutralized with 100 μl glacial acetic acid and ^{86}Rb or ^{36}Cl tracer activity was measured by β-scintillation counting. Uptakes were measured in the presence or absence of 20 μM bumetanide (Sigma-Aldrich) to calculate the bumetanide-sensitive (i.e. NKCC) portion of the K^+ or Cl^- uptake. NKCC1 flux is expressed in nanomoles of K^+ or Cl^- per oocyte per hour.

K^+ loss in *Xenopus laevis* oocytes

Groups of 25–28 oocytes in a 35 ml dish were pre-incubated overnight in modified L15 medium containing 2.5 μCi ml^{-1} $^{86}Rb^+$ at 16°C. Measurement of total $^{86}Rb^+$ at time zero involved the rapid washing of a group of 25–28 oocytes 4 times in ice-cold isosmotic saline (195–200 mosmol l^{-1}), then transferring them individually into glass vials for lysis and β-scintillation counting (see above). Measurement of hypertonic-stimulated (260–265 mosmol l^{-1}) K^+ loss was determined by incubating another two groups of 25–28 oocytes pre-loaded with $^{86}Rb^+$ in 50 ml of hypertonic saline containing 1 mM ouabain (± 20 μM bumetanide) for 1 h. After removal of the efflux solution, individual

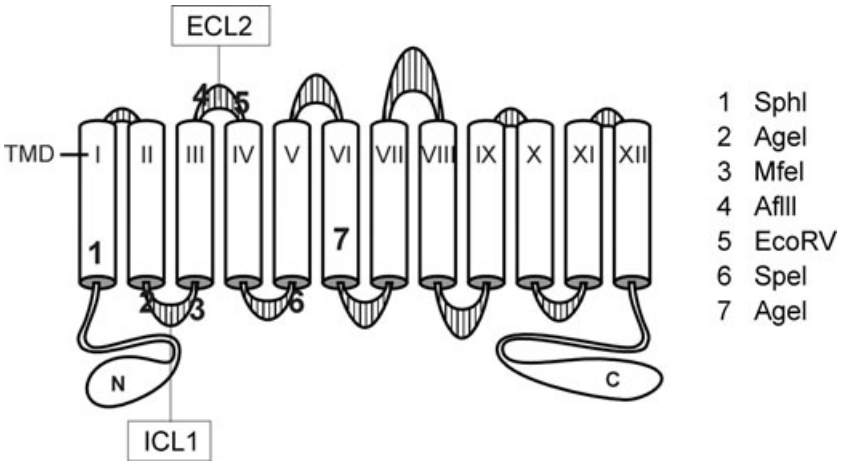

Figure 1. Schematic representation of the secondary structure of the Na^+–K^+–$2Cl^-$ cotransporter with the positions of the restriction sites used to create the various chimeras
TMD, transmembrane domain; ICL, intracellular loop; ECL, extracellular loop.

oocytes were then transferred to glass vials, lysed for 1 h with 200 μl 0.25 M NaOH, neutralized with 100 μl glacial acetic acid and ^{86}Rb tracer activity was measured by β-scintillation counting.

K^+ efflux in *Xenopus laevis* oocytes

Groups of 25–28 oocytes in a 35 ml dish were pre-incubated overnight in modified L15 medium containing 2.5 μCi ml^{-1} $^{86}Rb^+$ at 16°C. We created a holding/transfer device by removing the terminal 2 cm from a 5 ml plastic pipette tip and attaching a small screen/mesh (0.25 mm^2 holes) to the end to allow for easy solution exchange. Individual wells of a 24 well cell culture plate were filled with 1 ml of hypertonic saline or 1 ml of hypertonic K^+-free saline (K^+ replaced by an equivalent amount of Na^+). The transfer device was back-loaded with six oocytes in their overnight uptake solution and then transferred from well to well every minute for the first 4 min and every 2 min for the remaining 26 min. At the end of the 30 min efflux, the six oocytes were recovered and transferred to glass vials, lysed for 1 h with 200 μl 0.25 N NaOH, neutralized with 100 μl glacial acetic acid and ^{86}Rb tracer activity was measured by β-scintillation counting. Loss of $^{86}Rb^+$ was measured by transferring 300 μl of solution from each well into glass vials for β-scintillation counting. The amount of $^{86}Rb^+$ in the oocytes (in counts min^{-1}) was back-calculated for every time point and plotted on logarithmic scale as a function of time. Rate constant for efflux (slope), expressed in per minute, was determined after linear regression analysis.

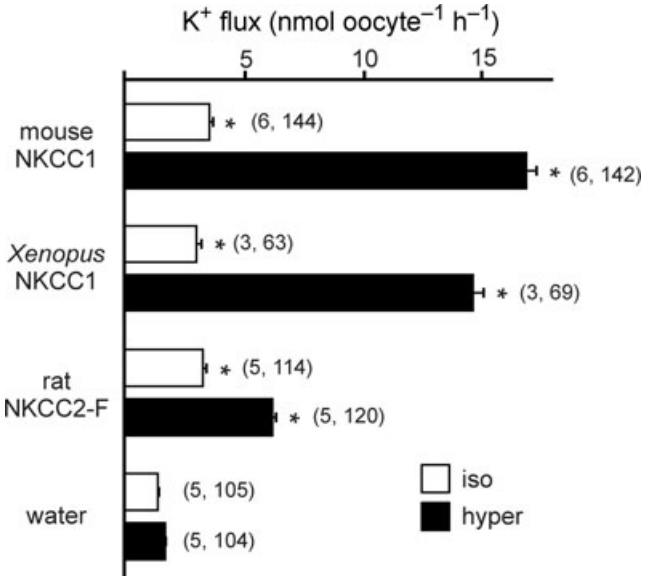

Figure 2. Functional analysis of mouse, frog and rat cation–chloride cotransport with ^{86}Rb (K^+) flux in *Xenopus laevis* oocytes
Water (50 nl) containing 15 ng of cRNA from wild-type mouse NKCC1, frog NKCC1 or rat NKCC2 (F variant) were injected on day 2. Oocytes injected with 50 nl of water only were used as baseline controls. K^+ flux was measured on day 5 in isosmotic (195 mosmol l^{-1}, open bars) and hyperosmotic (265 mosmol l^{-1}, filled bars) conditions. Bars represent mean ± S.E.M. (number of frogs, number of oocytes). Asterisk indicates highly significant difference ($P < 0.001$) between groups, relative to water-injected oocytes.

Statistical analysis

K^+ and Cl^- uptake were measured in individual oocytes by scintillation counting. Each wild-type and chimeric construct were tested multiple times. The results of each experimental group represented by 20–25 oocytes were pooled from different frogs tested on different days. Differences between groups were tested using one-way ANOVA, followed by multiple comparisons using the Student–Newman–Keuls, Bonferroni and Tukey's *post hoc* tests. $P > 0.05$ was considered to be non-significant, whereas $P < 0.001$ was considered to be very significant.

Results

When injected into *Xenopus laevis* oocytes, cRNA encoding mouse NKCC1 and rat NKCC2 yielded isotonic and hypertonic K^+ uptakes that were significantly higher than those of water-injected oocytes (Fig. 2). Levels of K^+ uptake under isosmotic conditions were similar for mouse NKCC1 and rat NKCC2. In contrast, hypertonicity stimulated NKCC1-mediated K^+ uptake to a much larger extent than NKCC2-mediated K^+ uptake (Fig. 2). Although, using the *Xenopus* oocyte expression system, we have observed some experimental variability in the absolute isotonic (3–6 nmol oocyte^{-1} h^{-1}) and hypertonic (12–20 nmol oocyte^{-1} h^{-1}) K^+ uptake values, the fold activation between the two osmotic conditions has always been greater than 3 for NKCC1 and less than 2 for NKCC2. As the K^+ uptake measured in water-injected oocytes was only minimally stimulated by hypertonicity, we cloned the frog cotransporter from oocytes. Interestingly, when over-expressed in oocytes, the osmotic fold activation for *Xenopus* NKCC1-mediated activity was 3.8, similar to the 3.6-fold activation of mouse NKCC1 (Fig. 2 and Table 1).

When ^{36}Cl was used to trace the movement of Cl^- through the transporters, an unusual behaviour was observed under hypertonicity. As shown in Fig. 3, the bumetanide-sensitive isosmotic and SPAK/WNK4-activated (Gagnon *et al.* 2006*b*) NKCC1 and NKCC2 fluxes both exhibited the characteristic $1K^+$:$2Cl^-$ stoichiometry. However, the bumetanide-sensitive Cl^- uptakes for NKCC1 and NKCC2 under hypertonicity were nearly the same as those observed under isosmotic conditions, respectively. This indicates that both NKCC1 and NKCC2 are exhibiting significant amounts of

Table 1. Fold activation of K^+ uptake by different wild-type and chimeric transporters under hypertonic (265 mosmol l^{-1}) *versus* isotonic (200 mosmol l^{-1}) conditions

NKCC1-like		NKCC2-like	
NKCC1 (*M.m.*)	**3.6**	NKCC2 (*R.n.*)	**1.9**
NKCC1 (*X.l.*)	**3.8**	Chimera 1	**1.9**
Chimera 2	**2.9**	Chimera 4	**1.1**
Chimera 3	**4.4**	Chimera 7	**2.0**
Chimera 5	**4.4**	Chimera 10	**1.5**
Chimera 6	**4.3**	Chimera 13	**2.1**
Chimera 8	**3.0**	Chimera 14	**2.0**
Chimera 9	**3.9**	Chimera 15	**2.1**
Chimera 11	**3.1**		
	Chimera 12	**1.2**	

Values are grouped as NKCC1-like (3- to 4-fold) or NKCC2-like (1- to 2-fold) behaviours. Wild-type cotransporters are indicated by initials of their latin names: *Musculus musculus* (*M.m.*), *Rattus norvegicus* (*R.n.*) and *Xenopus laevis (X.l)*. Note that chimera 12 is placed in the middle as it behaves like both NKCC1 and NKCC2.

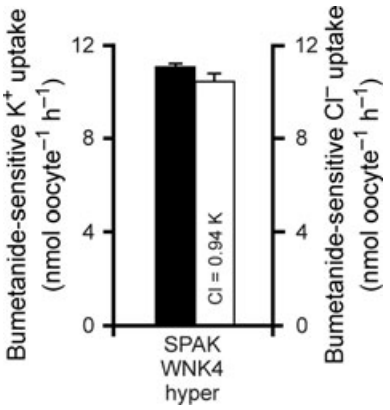

Figure 4. Hypertonic NKCC1-mediated K^+ and Cl^- uptakes in *Xenopus laevis* oocytes co-injected with SPAK and WNK4 kinases
Water (50 nl) containing 15 ng of cRNA of wild-type NKCC1 was injected on day 2. On day 3, 50 nl of water containing 10 ng of SPAK cRNA and 10 ng of WNK4 cRNA were injected. Bumetanide-sensitive K^+ (filled bars) and Cl^- (open bars) fluxes were measured on day 5 in hyperosmotic (265 mosmol l^{-1}) conditions. Bars represent mean ± S.E.M. (n = 20–25 oocytes).

bumetanide-sensitive K^+ uptake that is not matched by a 2-fold cotransport of Cl^-. To assess whether hypertonicity also affected the $1K^+$:$2Cl^-$ stoichiometry in NKCC1 stimulated by the kinases, we also performed parallel measurement of K^+ and Cl^- uptakes in oocytes co-injected with NKCC1, SPAK and WNK4 and exposed to hypertonicity. As shown in Fig. 4, hypertonicity also produced equivalent NKCC1-mediated K^+ and Cl^- uptake under kinase stimulation.

To demonstrate that the NKCC1-mediated K^+ uptake measured under hyperosmotic conditions represents K^+/K^+ exchange and not Na^+-independent K^+–Cl^- cotransport, we examined the requirement for *trans* K^+. As it is easier to manipulate external K^+, we determined the effect of external K^+ on K^+ efflux. In these experiments, oocytes were loaded overnight with ^{86}Rb, thoroughly washed, and the efflux of isotope was then measured. Figure 5*A* demonstrates that the majority of the K^+ loss is sensitive to 20 μM bumetanide (i.e. mediated by NKCC1). Washout kinetics were then performed to assess the role of external K^+ on K^+ efflux. In Fig. 5*B* the slope of a log-linear plot of K^+ efflux (cumulative counts per minute) *versus* time in hyperosmotic K^+-containing solution yielded a rate constant of -14.33×10^{-3} min^{-1}, which corresponds to a half-life of 69.7 min. In contrast, the slope of the K^+ efflux in a K^+-free solution was determined to be -2.84×10^{-3} min^{-1}, which corresponds to a half-life of 480 min.

The difference in cotransporter-mediated K^+ uptake was significantly larger in NKCC1 than NKCC2 (Fig. 3). This larger NKCC1 activation was not due to the regulatory N-terminal tails, as the N-terminal tail of NKCC1 attached to an NKCC2 backbone (chimera 1) produced a 1.9-fold

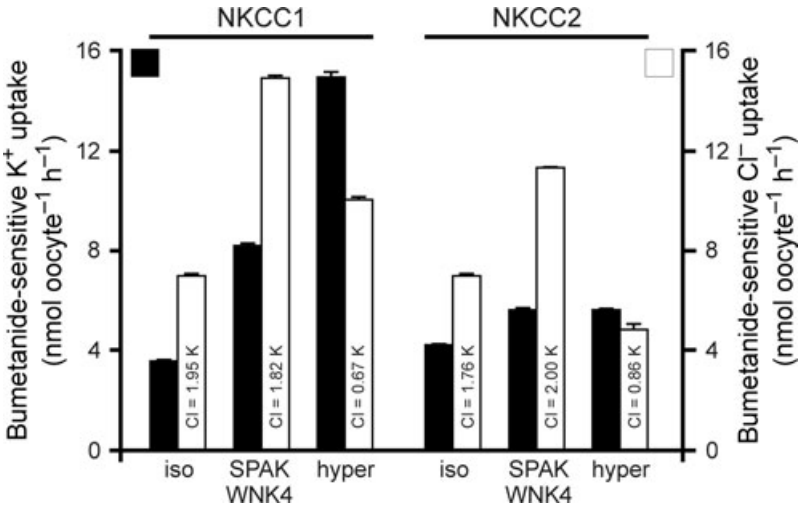

Figure 3. Functional analysis of wild-type mouse NKCC1 and wild-type rat NKCC2 with ^{86}Rb (K^+) and ^{36}Cl flux in *Xenopus laevis* oocytes
Water (50 nl) containing 15 ng of cRNA of wild-type NKCC1 or rat NKCC2 (F variant) was injected on day 2. Water (50 nl) containing 10 ng of SPAK cRNA and 10 ng of WNK4 cRNA was injected in some groups on day 3. Bumetanide-sensitive K^+ (filled bars) and Cl^- (open bars) fluxes were measured on day 5 in isosmotic (195 mosmol l^{-1}), SPAK/WNK4 kinase-stimulated and hyperosmotic (265 mosmol l^{-1}) conditions. Bars represent mean ± S.E.M. (n = 20–25 oocytes).

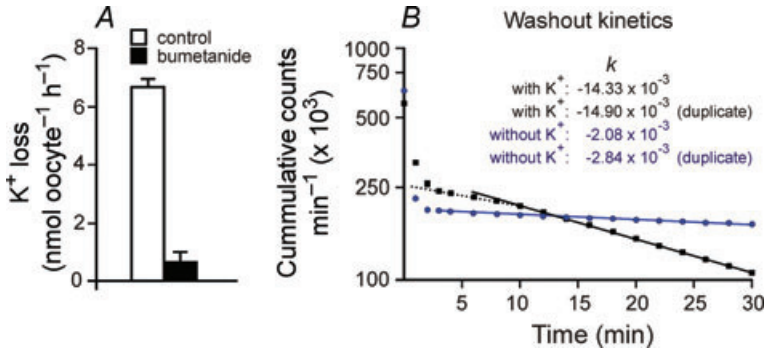

Figure 5. NKCC1-mediated K^+ loss in oocytes under hypertonicity
A, K^+ loss per oocyte per hour in the absence and presence of 20 μM bumetanide. *B*, log-linear plot of ^{86}Rb content (in counts min^{-1}) in oocytes as a function of time. The slopes of potassium-free (filled circles) and potassium-containing (filled squares) represent the rate constants of K^+ efflux, expressed in min^{-1}. The initial rapid and non-linear component represents the washout of the external ^{86}Rb, that is the radioactivity which is carried over with the oocytes when the device is moved from the uptake solution to the washout solutions. The dashed line represents an initially slower linear component of K^+ efflux which indicates the lag-time of NKCC1 activation by hypertonicity when the oocytes are transferred from the isotonic ^{86}Rb-containing L15 medium to the hypertonic efflux medium.

activation, which is similar to wild-type NKCC2, whereas the N-terminal tail of NKCC2 attached to NKCC1 (chimera 2) resulted in a 2.9-fold activation, comparable to wild-type NKCC1 (Fig. 6, Table 1).

In order to identify the region(s) of NKCC1 responsible for the 3- to 4-fold activation of K^+ uptake, we began by creating a set of chimeras which involved transposing the cotransporter molecules at the sixth transmembrane domain (TMD6). Chimeras 3 and 4 show that the fold activation phenotype was contained within the first half of the NKCC1 molecule (Fig. 6, Table 1). We then created additional chimeras by progressively removing regions of NKCC1 and substituting them with NKCC2 sequences. Chimeras 5 and 6 show that the residues of NKCC1 that are responsible for the fold activation in K^+ uptake exist within the first three transmembrane domains and the second extracellular loop (Fig. 7, Table 1). However, once the second extracellular loop was replaced with its corresponding NKCC2 sequence (chimera 7), the hypertonic fold activation in K^+ uptake was significantly reduced (Fig. 7, Table 1). In Fig. 6, we demonstrated no participation of the N-terminus in the hyperosmotic fold activation in K^+ uptake. In Fig. 8*A*, we illustrate by amino acid alignment that the first transmembrane domain (TMD1) and TMD3 are identical between NKCC1 and NKCC2. In order to demonstrate that the first extracellular loop (ECL1), TMD2, the first intracellular loop (ICL1) and ECL2 from NKCC1 are sufficient to elicit the hyperosmotic fold activation in K^+ uptake, we created a chimera that has the N-terminal tail, the 1 and 3–12 transmembrane domains of NKCC2, but the ECL1, TMD2, ICL1 and ECL2 of NKCC1 (chimera 8) and showed

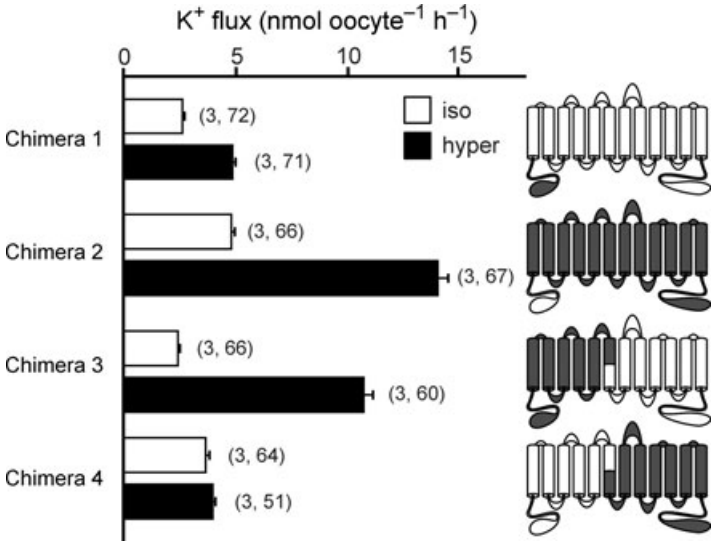

Figure 6. NKCC1–NKCC2 chimeras were tested by functional analysis of ^{86}Rb (K^+) flux in *Xenopus laevis* oocytes
Water (50 nl) containing 15 ng of cotransporter cRNA was injected on day 2. K^+ flux was measured on day 5 in isosmotic (195 mosmol l^{-1}, open bars) and hyperosmotic (265 mosmol l^{-1}, filled bars) conditions. Cartoon colouring illustrates the contribution of NKCC1 (grey) to NKCC2 (white) in each chimera. Bars represent mean ± S.E.M. (number of frogs, number of oocytes).

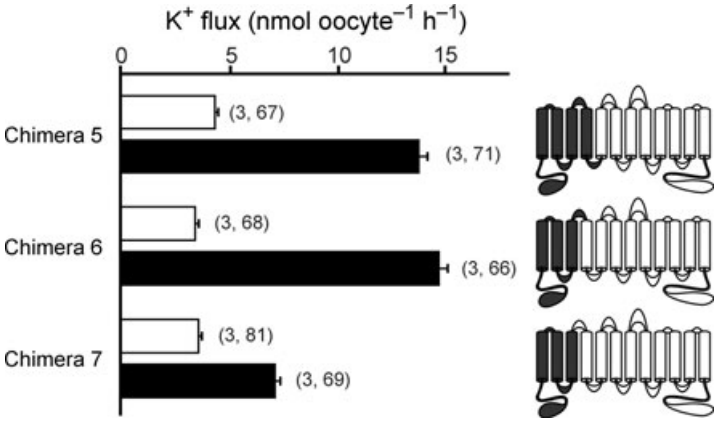

Figure 7. NKCC1–NKCC2 chimeras were tested by functional analysis of ^{86}Rb (K^+) flux in *Xenopus laevis* oocytes
Water (50 nl) containing 15 ng of cotransporter cRNA was injected on day 2. K^+ flux was measured on day 5 in isosmotic (195 mosmol l^{-1}, open bars) and hyperosmotic (265 mosmol l^{-1}, filled bars) conditions. Cartoon colouring illustrates the contribution of NKCC1 (grey) to NKCC2 (white) in each chimera. Bars represent mean ± S.E.M. (number of frogs, number of oocytes).

that it behaved similar to wild-type NKCC1 (Fig. 8*B*, Table 1). To address the individual role of each of these components, we first changed a glutamine residue into a glutamic acid (Q308E) by site-directed mutagenesis, as it was the only non-conserved residue within ICL1 (Fig. 8*B*, chimera 9). We observed a hypertonic 3.9-fold activation similar to wild-type NKCC1-mediated K^+ uptake (Fig. 8*B*, Table 1). Replacement of the first intracellular loop in NKCC2 with ICL1 from NKCC1 (chimera 10) did not significantly alter the isotonic, but significantly reduced the hypertonic-stimulated K^+ uptake, thus resulting in only a 1.5-fold activation similar to wild-type NKCC2 (Fig. 8*B*, Table 1). Although, replacement of the second extracellular loop of NKCC2 with ECL2 of NKCC1 (chimera 11) resulted in lower absolute isotonic and hypertonic K^+ uptakes, the characteristic 3-fold activation between hypertonic and isotonic was maintained (Fig. 8*B*, Table 1). Interestingly, replacement of ICL1 and ECL2 in NKCC2 with the corresponding regions of NKCC1 (chimera 12) resulted in a hypertonic-stimulated K^+ uptake similar to wild-type NKCC1, but also a stimulated K^+ uptake under isotonic conditions which eliminated the fold activation (Fig. 8*B*, Table 1).

Figure 9*A* illustrates a protein alignment of the second extracellular loop (ECL2) between mouse NKCC1 and rat NKCC2. As any of these non-conserved residues might have a role in the 3-fold activation in K^+ uptake observed with chimera 8 (Fig. 8*B*, Table 1), we used

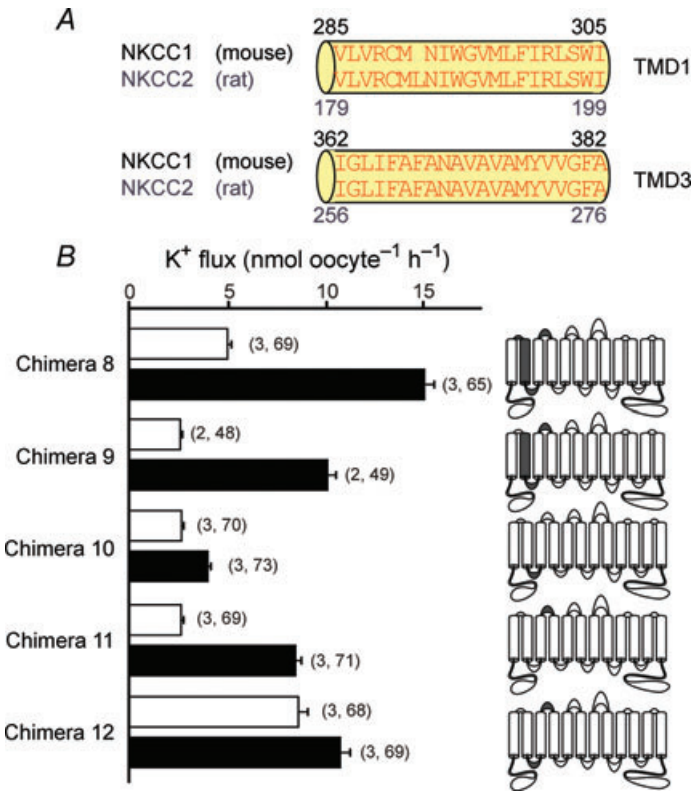

Figure 8. K^+ uptake in NKCC1–NKCC2 chimeras identify TMD2, ICL1, and ECL2 as domains involved in NKCC1 activation by hypertonicity
A, alignment of the first and third transmembrane domains (TMD1 and TMD3, respectively) of mouse NKCC1 and rat NKCC2 (F variant) illustrating identical amino acid sequences. *B*, functional analysis of NKCC1–NKCC2 chimeras by ^{86}Rb (K^+) flux in *Xenopus laevis* oocytes. Water (50 nl) containing 15 ng of cotransporter cRNA was injected on day 2. K^+ flux was measured on day 5 in isosmotic (195 mosmol l^{-1}, open bars) and hyperosmotic (265 mosmol l^{-1}, filled bars) conditions. Cartoon colouring illustrates the contribution of NKCC1 (grey) to NKCC2 (white) in each chimera. Bars represent mean ± S.E.M. (number of frogs, number of oocytes).

site-directed mutagenesis to convert the mouse NKCC1 ECL2 histidine at position 393 into a serine (H393S, chimera 13), the glutamic acid at position 398 into a proline (E398P, chimera 14) and the isoleucine at position 399 into a threonine (I399T, chimera 15) in the chimera 8 background (Fig. 9*A*). The mutation of each of these non-conserved residues resulted in fold activations similar to wild-type NKCC2 (Fig. 9*B*, Table 1).

Discussion

We and others have shown that NKCC1-mediated K^+ uptake is stimulated several-fold under hypertonicity (Geck & Pfeiffer, 1985; Whisenant *et al.* 1991; O'Donnell *et al.* 1995; Lytle & Forbush, 1996; Lytle, 1997; Piechotta *et al.* 2003). Our laboratory has used the *Xenopus laevis* oocyte expression system to study the regulation of heterologously expressed cotransporters because the functional activity of the native cotransporter is minimal (Piechotta *et al.* 2003; Gagnon *et al.* 2006*b*, 2007). Previous studies demonstrated only a 1.5-fold activation in the hypertonic stimulation of native *Xenopus* NKCC1-mediated K^+ uptake (Suvitayavat *et al.* 1994). We confirmed in our water-injected oocytes, a 1.3-fold activation in NKCC-mediated K^+ uptake (Fig. 2). The lack of hypertonic sensitivity of the *Xenopus* NKCC1 prompted us to clone the frog cotransporter and identify structural features that might account for the differential osmotic sensitivities. However, we observed no significant difference in K^+ uptake between over-expressed frog and mouse NKCC1 in *Xenopus* oocytes. This suggests that the oocytes have a limited number of cotransporters and that most of these cotransporters are already active under isotonic conditions. Since we could not use the amphibian cotransporter to characterize the hypertonic fold activation of mouse NKCC1, we used a variant of NKCC2 that was previously shown to have a reduced sensitivity to osmolarity (Gimenez & Forbush, 2005). In Fig. 2, we confirmed that rat NKCC2 (F variant) has less than a 2-fold activation in hypertonic-stimulated K^+ uptake.

An interesting observation of this study was the demonstration that under isosmotic conditions with or without co-expression of SPAK and WNK4 kinases, the measured Cl^- to K^+ ratio of NKCC1 was close to 2, consistent with NKCC1 functioning as a Na^+–K^+–$2Cl^-$ cotransporter. In contrast, while the K^+ uptake was significantly stimulated under hypertonicity, the Cl^- uptake was stimulated to a much lesser degree making the Cl^- to K^+ ratio approximately 1. This observation indicates that a large fraction of K^+ moved independently of Cl^-. Such behaviour has been recognized in the past as a partial reaction of the cotransporter which supports K^+/K^+ exchange (Russell, 2000). To our knowledge, this is the first demonstration of K^+/K^+ (and Cl^-/Cl^-) exchange favoured under hypertonic stimulation of the cotransporter. Partial reactions (i.e. K^+/K^+ exchange) due to reloading of the transporter might be related to the increase in intracellular Na^+ and Cl^- concentrations associated with cell shrinkage. K^+/K^+ exchange was first demonstrated in duck red blood cells under complete absence of external Na^+ (Schmidt & McManus, 1977*b*; Lauf *et al.* 1987). Interestingly, this exchange was both activated and inhibited by all conditions known to affect Na^+–K^+–$2Cl^-$ cotransport. More importantly, this exchange necessitates the presence of internal Na^+ and external Cl^-, requirements that suggested a strict order of ion binding (Lytle *et al.* 1998). In this ordered binding

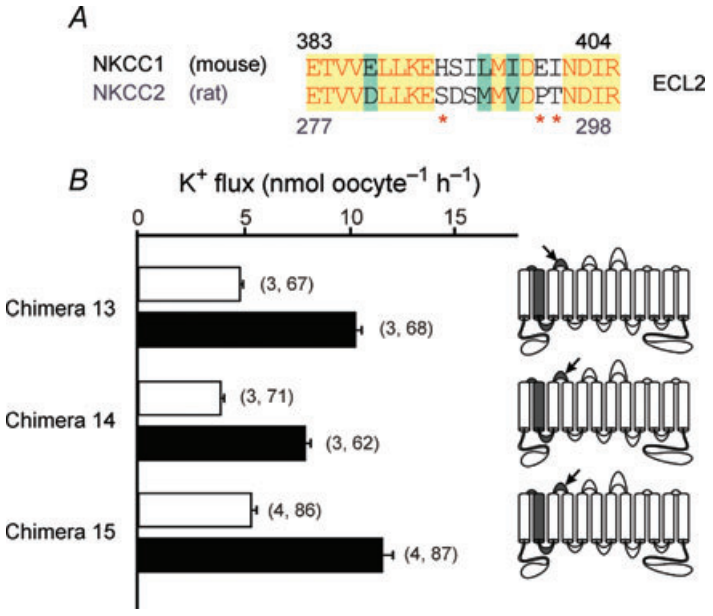

Figure 9. Effect of single residue mutations in ECL2 on K^+ uptake
A, alignment of the second extracellular loop (ECL2) of mouse NKCC1 and rat NKCC2. Red letters on yellow background indicate identical residues, black letters on green background indicate conserved residues and black letters on white background indicate non-conserved residues. Red asterisks denote which residues were altered by site-directed mutagenesis. *B*, functional analysis of NKCC1–NKCC2 chimeras with ^{86}Rb (K^+) flux in *Xenopus laevis* oocytes. Water (50 nl) containing 15 ng of cotransporter cRNA was injected on day 2. K^+ flux was measured on day 5 in isosmotic (195 mosmol l^{-1}, open bars) and hyperosmotic (265 mosmol l^{-1}, filled bars) conditions. Cartoon colouring illustrates the contribution of NKCC1 (grey) to NKCC2 (white) in each chimera. Arrows indicate the relative position of the site-directed mutations identified by red asterisks in *A*. Bars represent mean ± S.E.M. (number of frogs, number of oocytes).

model, the cotransporter binds a Na^+, Cl^-, K^+ and then a second Cl^- ion. After the transporter translocates, it releases the ions in the same order they were bound, namely a Na^+, a Cl^- and a K^+ ion (see Fig. 10). However, under hypertonic conditions, rather than going full circle and releasing the second Cl^-, the cotransporter reverses and reloads a K^+, Cl^- and Na^+ ion. The net effect of this reversal is an exchange of K^+ and Cl^-. These simultaneous K^+/K^+ and Cl^-/Cl^- exchanges are the basis for our observed K^+:Cl^- ratio of approximately 1. This partial reaction does not, however, require absence of external Na^+, as bumetanide-sensitive unidirectional influx of K^+ greater than Na^+ can also be observed under normal ionic concentrations (Schmidt & McManus, 1977*b*). Note, however, that K^+/K^+ exchange requires the presence of K^+ on both sides of the membrane, in contrast to true Na^+–K^+–2Cl^- cotransport or Na^+-independent K^+–2Cl^- cotransport. This was verified in efflux studies presented in Fig. 5, where K^+ efflux was significantly reduced in a K^+-free hypertonic solution.

Unlike the cotransport of ions that is accompanied by obligatory water movement, K^+/K^+ and Cl^-/Cl^- exchange does not result in a net movement of ions and therefore does not create a net water movement. This might be why most cells when exposed to high external osmolarities will shrink but not undergo regulatory volume increase (for reviews, see Hoffmann & Simonsen, 1989; Hoffmann *et al.* 2009). However, when cells are first exposed to a hypotonic environment, they swell and undergo regulatory volume decrease. When returned to their initial tonicity, they will shrink and then undergo regulatory volume increase (for reviews, see Hoffmann & Simonsen, 1989; Hoffmann *et al.* 2009). The difference between these two situations is that shrinkage under hypertonicity stimulates K^+/K^+ exchange instead of Na^+–K^+–2Cl^- cotransport, *versus* shrinkage post regulatory volume decrease stimulates true cotransport. These distinct behaviours could be due to different levels in intracellular Cl^- (i.e. relatively high Cl^- in cells initially exposed to hypertonicity, whereas reduced intracellular Cl^- post regulatory volume decrease). When NKCC1 functions in true cotransport mode, the vectorial movement of Na^+, K^+ and Cl^- is associated with an obligatory movement of water. For epithelial cells that transfer salts from one side of the epithelium to the other, this means that in order to maintain their cell volume, the intake of water on one side must be matched by a loss of water on the other side. In agreement with this concept, polarized choroid plexus epithelial cells exposed to bumetanide shrink, as NKCC1 inhibition creates an imbalance between water intake at the apical membrane and water loss at the basolateral membrane (Wu *et al.* 1998).

NKCC function depends upon phosphorylation of its cytoplasmic N-terminus (Lytle & Forbush, 1992; Lytle, 1997). Indeed, several sites of phosphorylation that are relevant to cotransport function have been identified within the amino-termini of both NKCC1 and NKCC2 (Lytle & Forbush, 1992; Darman & Forbush, 2002; Gimenez & Forbush, 2005; Vitari *et al.* 2006; Gagnon *et al.* 2007). Exactly how these phosphorylation events regulate cotransporter activity is still unclear. However, we now know that these sites are phosphorylated by two kinases (SPAK and OSR1) which bind upstream at RF*x*[V/I] docking sites (Piechotta *et al.* 2002; Dowd & Forbush, 2003) and we have shown that these kinases participate, at least partially, in the hypertonic activation of NKCC1 (Gagnon *et al.* 2006*b*). As there is only 29% conservation in the amino termini between the two isoforms, we first postulated that the difference between the two cotransporters might be encoded in this cytoplasmic domain and thus replaced the 279 residue amino-terminus of the mouse NKCC1 with the 172 residue amino-terminus of the rat NKCC2. Interestingly, we found that the smaller amino termini of NKCC2 did not inhibit the fold activation of NKCC1, nor did the larger amino termini of NKCC1 transfer osmotic sensitivity to NKCC2. Although the phosphorylation of the N-terminus is a pre-requisite for cotransporter function, the different levels of hypertonic-stimulated fold activation observed between NKCC1 and NKCC2 are therefore probably due to structural differences in their transmembrane cores.

Our experiments with successive chimeric iterations allowed us to eliminate the second half of the protein and

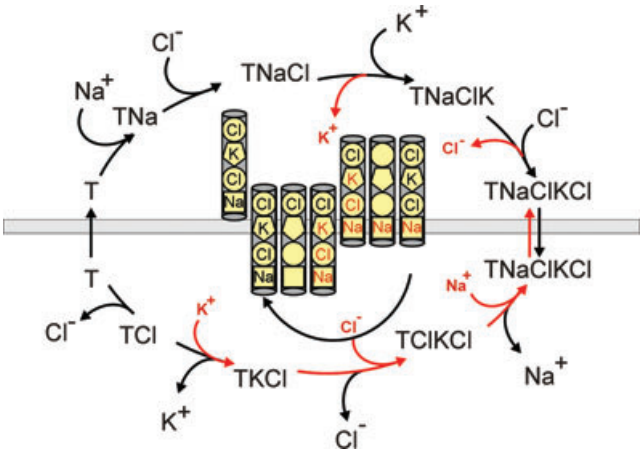

Figure 10. Glide symmetry model of NKCC1 as proposed by Lytle *et al*. (1998)
Under isotonic conditions, empty NKCC1 binds in the order: one Na^+, one Cl^-, one K^+ and a second Cl^-. After translocation, NKCC1 releases in the same order: the Na^+, the first Cl^-, the K^+ and the second Cl^-.Then, the cotransporter translocates empty and the cycle repeats. Under hypertonicity, partial reactions occur with the transporter reversing inside prior to unloading the second Cl^- and outside prior to unloading the Na^+. As a result, these partial cycles exchange external K^+ and Cl^- for internal K^+ and Cl^-, i.e. K^+/K^+ and Cl^-/Cl^- exchanges. Externally loaded ions are represented in black, internally loaded ions are represented in red.

to reduce the area of interest to the first intracellular loop (ICL1), the second transmembrane domain (TMD2) and the second extracellular loop (ECL2) of NKCC1. When we substituted NKCC1 TMD2 and ECL2 with corresponding regions in NKCC2, we observed a reduction in the fold activation from 3.9 to 1.5, indicating their importance in the hypertonic sensitivity of the cotransporter. Indeed, substitution of just the second extracellular loop of NKCC2 with the corresponding NKCC1 segment maintained the 3-fold activation in hypertonic-stimulated K^+ uptake. Only one chimera produced an unexpected behaviour that resembled both NKCC1 and NKCC2. Chimera 12 produced hypertonic K^+ uptake that was similar to that mediated by wild-type NKCC1, but the nearly equivalent amount of uptake under isosmotic conditions produced a 1.2-fold activation that was similar to NKCC2. These data suggest that an interaction between ICL1, TMD2 and ECL2 is responsible for regulating the isotonic activity of the cotransporter. The possibility of ICL1 and TMD2 interacting is supported by recent studies that proposed a model where, rather than being cytosolic, ICL1 is partially embedded in the plasma membrane (Gimenez & Forbush, 2007). Furthermore, previous studies using a similar chimeric strategy have demonstrated the importance of TMD2 and ICL1 in defining cotransporter affinities for Na^+, K^+ and Cl^- (Isenring & Forbush, 1997; Isenring *et al.* 1998*a*,*b*; Gimenez & Forbush, 2007).

Based on the results obtained with chimeras 8–11, we produced single point mutations in the ECL2 of chimera 8, thereby partially converting NKCC1 ECL2 into NKCC2 ECL2 reversing the hypertonic fold activation, highlighting the importance of H393, E399 and I400 in ECL2 to the osmotic sensitivity of NKCC1. Note that in the shark *versus* human NKCC1 study (Isenring *et al.* 1998*b*), chimeras were created with a junction point located at the beginning of TMD3. These chimeras showed partial recapitulation of the affinities of their parent molecule, indicating that TMD2 and ICL1 could not fully account for these affinities. It is therefore possible that ECL2 was the missing component for the full recapitulation. How the loops interact with the core proteins and how hypertonicity affects this interaction are questions that cannot be answered without crystallographic resolution of the cotransporter structures.

In summary, we have shown that the molecular determinants for the osmotic sensitivity of NKCC1 involve some interaction between the first intracellular, second transmembrane domain and the second extracellular loop of the cotransporter. Our experiments specifically highlight the significance of the second extracellular loop in the hypertonic activation of NKCC1. We have also demonstrated that hypertonicity stimulates NKCC1-mediated K^+ uptake that is not matched by Cl^- movements, therefore probably representing K^+/K^+ and Cl^-/Cl^- exchange. As vectorial movement of Na^+, K^+ and Cl^- ions through the cotransporter is not stimulated by hypertonicity, the physiological relevance of the hyperosmotic sensitivity of the cotransporter remains unknown.

References

Alvarez-Leefmans FJ (2009). Chloride transporters in presynaptic inhibition, pain and neurogenic inflammation. In *Physiology and Pathology of Chloride Transporter and Channels in the Nervous System: From Molecules to Diseases*, ed. Alvarez-Leefmans FJ & Delpire E, pp. 439–470. Academic Press, London.

Alvarez-Leefmans FJ, Gamiño SM, Giraldez F & Nogueron I (1988). Intracellular chloride regulation in amphibian dorsal root ganglion neurons studied with ion-selective microelectrodes. *J Physiol* **406**, 225–246.

Dan I, Watanabe NM & Kusumi A (2001). The Ste20 group kinases as regulators of MAP kinase cascades. *Trends Cell Biol* **11**, 220–230.

Darman RB & Forbush B (2002). A regulatory locus of phosphorylation in the N terminus of the Na-K-Cl cotransporter, NKCC1. *J Biol Chem* **277**, 37542–37550.

Delpire E (2009). The mammalian family of Sterile20p-like protein kinases. *Pflügers Arch* **458**, 953–967.

Delpire E, Lu J, England R, Dull C & Thorne T (1999). Deafness and imbalance associated with inactivation of the secretory Na-K-2Cl co-transporter. *Nat Genet* **22**, 192–195.

Douglas IJ & Brown PD (1996). Regulatory volume increase in rat lacrimal gland acinar cells. *J Membr Biol* **150**, 209–217.

Dowd BF & Forbush B (2003). PASK (proline-alanine-rich STE20-related kinase), a regulatory kinase of the Na-K-Cl cotransporter (NKCC1). *J Biol Chem* **278**, 27347–27353.

Gagnon KB, England R & Delpire E (2006*a*). Characterization of SPAK and OSR1, regulatory kinases of the Na-K-2Cl cotransporter. *Mol Cell Biol* **26**, 689–698.

Gagnon KB, England R & Delpire E (2006*b*). Volume sensitivity of cation-chloride cotransporters is modulated by the interaction of two kinases: SPAK and WNK4. *Am J Physiol Cell Physiol* **290**, C134–C142.

Gagnon KB, England R & Delpire E (2007). A single binding motif is required for SPAK activation of the Na-K-2Cl cotransporter. *Cell Physiol Biochem* **20**, 131–142.

Geck P & Pfeiffer B (1985). $Na^+ + K^+ + 2Cl^-$ cotransport in animal cells – its role in volume regulation. *Ann N Y Acad Sci* **456**, 166–182.

Geck P, Pietrzyk C, Burckhardt B-C, Pfeiffer B & Heinz E (1980). Electrically silent cotransport of Na^+, K^+ and Cl^- in Ehrlich cells. *Biochim Biophys Acta* **600**, 432–447.

Gimenez I & Forbush B (2005). Regulatory phosphorylation sites in the NH_2 terminus of the renal Na-K-Cl cotransporter (NKCC2). *Am J Physiol Renal Physiol* **289**, F1341–F1345.

Gimenez I & Forbush B (2007). The residues determining differences in ion affinities among the alternative splice variants F, A, and B of the mammalian renal Na-K-Cl cotransporter (NKCC2). *J Biol Chem* **282**, 6540–6547.

Haas M, McBrayer D & Lytle C (1995). $[Cl^-]_i$-dependent phosphorylation of the Na-K-Cl cotransport protein of dog tracheal epithelial cells. *J Biol Chem* **270**, 28955–28961.

Hoffmann EK, Lambert IH & Pedersen SF (2009). Physiology of cell volume regulation in vertebrates. *Physiol Rev* **89**, 193–277.

Hoffmann EK & Simonsen EK (1989). Membrane mechanisms in volume and pH regulation in vertebrate cells. *Physiol Rev* **69**, 315–382.

Isenring P & Forbush BI (1997). Ion and bumetanide binding by the Na-K-2Cl cotransporter: importance of transmembrane domains. *J Biol Chem* **272**, 24556–24562.

Isenring P, Jacoby SC, Chang J & Forbush BI (1998*a*). Mutagenic mapping of the Na-K-Cl cotransporter for domains involved in ion transport and bumetanide binding. *J Gen Physiol* **112**, 549–558.

Isenring P, Jacoby SC & Forbush BI (1998*b*). The role of transmembrane domain 2 in cation transport by the Na-K-Cl cotransporter. *Proc Natl Acad Sci USA* **95**, 7179–7184.

Kaplan MR, Plotkin MD, Lee W-S, Xu Z-C, Lytton J & Hebert SC (1996). Apical localization of the Na-K-2Cl cotransporter, rBSC1, on rat thick ascending limbs. *Kidney Int* **49**, 40–47.

Klein JD, Lamitina ST & O'Neill WC (1999). JNK is a volume-sensitive kinase that phosphorylates the Na-K-2Cl cotransporter *in vitro*. *Am J Phyiol Cell Physiol* **46**, C425–C431.

Kurihara K, Nakanishi N, Moore-Hoon ML & Turner RJ (2002). Phosphorylation of the salivary Na^+-K^+-$2Cl^-$ cotransporter. *Am J Physiol Cell Physiol* **282**, C817–C823.

Lauf PK, McManus TJ, Haas M, Forbush B 3rd, Duhm J, Flatman PW, Saier MH Jr & Russell JM (1987). Physiology and biophysics of chloride and cation cotransport across cell membranes. *Fed Proc* **46**, 2377–2394.

Liedtke CM (1989). Adrenergic regulation of Na-Cl cotransport human airway epithelium. *Am J Physiol Lung Cell Moll Physiol* **257**, L125–L129.

Lytle C (1997). Activation of the avian erythrocyte Na-K-Cl cotransport protein by cell shrinkage, cAMP, fluoride, and calyculin-A involves phosphorylation at common sites. *J Biol Chem* **272**, 15069–15077.

Lytle C & Forbush BI (1992). The Na-K-Cl cotransport protein of shark rectal gland. II. regulation by direct phosphorylation. *J Biol Chem* **267**, 25438–25443.

Lytle C & Forbush BI (1996). Regulatory phosphorylation of the secretory Na-K-Cl cotransporter: modulation by cytoplasmic Cl. *Am J Physiol Cell Physiol* **270**, C437–C448.

Lytle C, McManus TJ & Haas M (1998). A model of Na-K-2Cl cotransport based on ordered ion binding and glide symmetry. *Am J Physiol Cell Physiol* **274**, C299–C309.

Matthews JB, Smith JA, Tally KJ, Awtrey CS, Nguyen H, Rich J & Madara JL (1994). Na-K-2Cl cotransport in intestinal epithelial cells. Influence of chloride efflux and F-actin on regulation of cotransporter activity and bumetanide binding. *J Biol Chem* **269**, 15703–15709.

Moriguchi T, Urushiyama S, Hisamoto N, Iemura SI, Uchida S, Natsume T, Matsumoto K & Shibuya H (2006). WNK1 regulates phosphorylation of cation-chloride-coupled cotransporters via the STE20-related kinases, SPAK and OSR1. *J Biol Chem* **280**, 42685–42693.

O'Donnell ME, Martinez A & Sun D (1995). Endothelial Na-K-Cl cotransport regulation by tonicity and hormones: phosphorylation of cotransport protein. *Am J Physiol Cell Physiol* **269**, C1513–C1523.

Ozawa T, Saito Y & Nishiyama A (1988). Mechanism of uphill chloride transport of the mouse lacrimal acinar cells: studies with Cl^--sensitive microelectrode. *Pflugers Arch* **412**, 509–515.

Piechotta K, Garbarini NJ, England R & Delpire E (2003). Characterization of the interaction of the stress kinase SPAK with the Na^+-K^+-$2Cl^-$ cotransporter in the nervous system: evidence for a scaffolding role of the kinase. *J Biol Chem* **278**, 52848–52856.

Piechotta K, Lu J & Delpire E (2002). Cation-chloride cotransporters interact with the stress-related kinases SPAK and OSR1. *J Biol Chem* **277**, 50812–50819.

Plotkin MD, Kaplan MR, Peterson LN, Gullans SR, Hebert SC & Delpire E (1997). Expression of the Na^+-K^+-$2Cl^-$ cotransporter BSC2 in the nervous system. *Am J Physiol Cell Physiol* **272**, C173–C183.

Reisert J, Lai J, Yau KW & Bradley J (2005). Mechanism of the excitatory Cl^- response in mouse olfactory receptor neurons. *Neuron* **45**, 553–561.

Russell JM (2000). Sodium-potassium-chloride cotransport. *Physiol Rev* **80**, 211–276.

Sato K, Kang WH, Saga K & Sato KT (1989). Biology of sweat glands and their disorders. I. Normal sweat gland function. *J Am Acad Dermatol* **20**, 537–563.

Schmidt WF 3rd & McManus TJ (1977*a*). Ouabain-insensitive salt and water movements in duck red cells. I. Kinetics of cation transport under hypertonic conditions. *J Gen Physiol* **70**, 59–79.

Schmidt WF 3rd & McManus TJ (1977*b*). Ouabain-insensitive salt and water movements in duck red cells. II. Norepinephrine stimulation of sodium plus potassium cotransport. *J Gen Physiol* **70**, 81–97.

Sung K-W, Kirby M, McDonald MP, Lovinger DM & Delpire E (2000). Abnormal $GABA_A$-receptor mediated currents in dorsal root ganglion neurons isolated from Na-K-2Cl cotransporter null mice. *J Neurosci* **20**, 7531–7538.

Suvitayavat W, Palfrey HC, Haas M, Dunham PB, Kalmar F & Rao MC (1994). Characterization of the endogenous Na^+-K^+-$2Cl^-$ cotransporter in *Xenopus* oocytes. *Am J Physiol Cell Physiol* **266**, C284–C292.

Villa F, Goebel J, Rafiqi FH, Deak M, Thastrup J, Alessi DR & van Aalten DMF (2007). Structural insights into the recognition of substrates and activators by the OSR1 kinase. *EMBO Rep* **8**, 839–845.

Vitari AC, Thastrup J, Rafiqi FH, Deak M, Morrice NA, Karlsson HK & Alessi DR (2006). Functional interactions of the SPAK/OSR1 kinases with their upstream activator WNK1 and downstream substrate NKCC1. *Biochem J* **397**, 223–231.

Whisenant N, Zhang B-X, Khademazad M, Loessberg P & Muallem S (1991). Regulation of Na-K-2Cl cotransport in osteoblasts. *Am J Physiol Cell Physiol* **261**, C433–C440.

Wong JA, Gosmanov AR, Schneider EG & Thomason DB (2001). Insulin-independent, MAPK-dependent stimulation of NKCC activity in skeletal muscle. *Am J Physiol Regul Integr Comp Physiol* **281**, R561–R571.

Wu Q, Delpire E, Hebert SC & Strange K (1998). Functional demonstration of Na-K-2Cl cotransporter activity in isolated, polarized choroid plexus cells. *Am J Physiol Cell Physiol* **275**, C1565–C1572.

Author contributions

K.B.G. and E.D. contributed to the design, implementation and analysis of the experiments, wrote and approved the final revision of the manuscript.

Acknowledgements

We would like to thank Ghali Abdelmessih for his help in the husbandry and surgery of the *Xenopus laevis* frogs, and Kerri Rios for her technical assistance in creating some of the mutants and preparing the DNA for transcription. This work was supported by the National Institutes of Health grant GM074771to E.D.